5 September 2002

International weekly journal of science

nature

www.naturejpn.com

Seismic super-swarm

Stresses and strains beneath an island volcano

Safer drug design
Antidotes to order

Fighting terrorism
The US research agenda

Antibody production
Origins of diversity

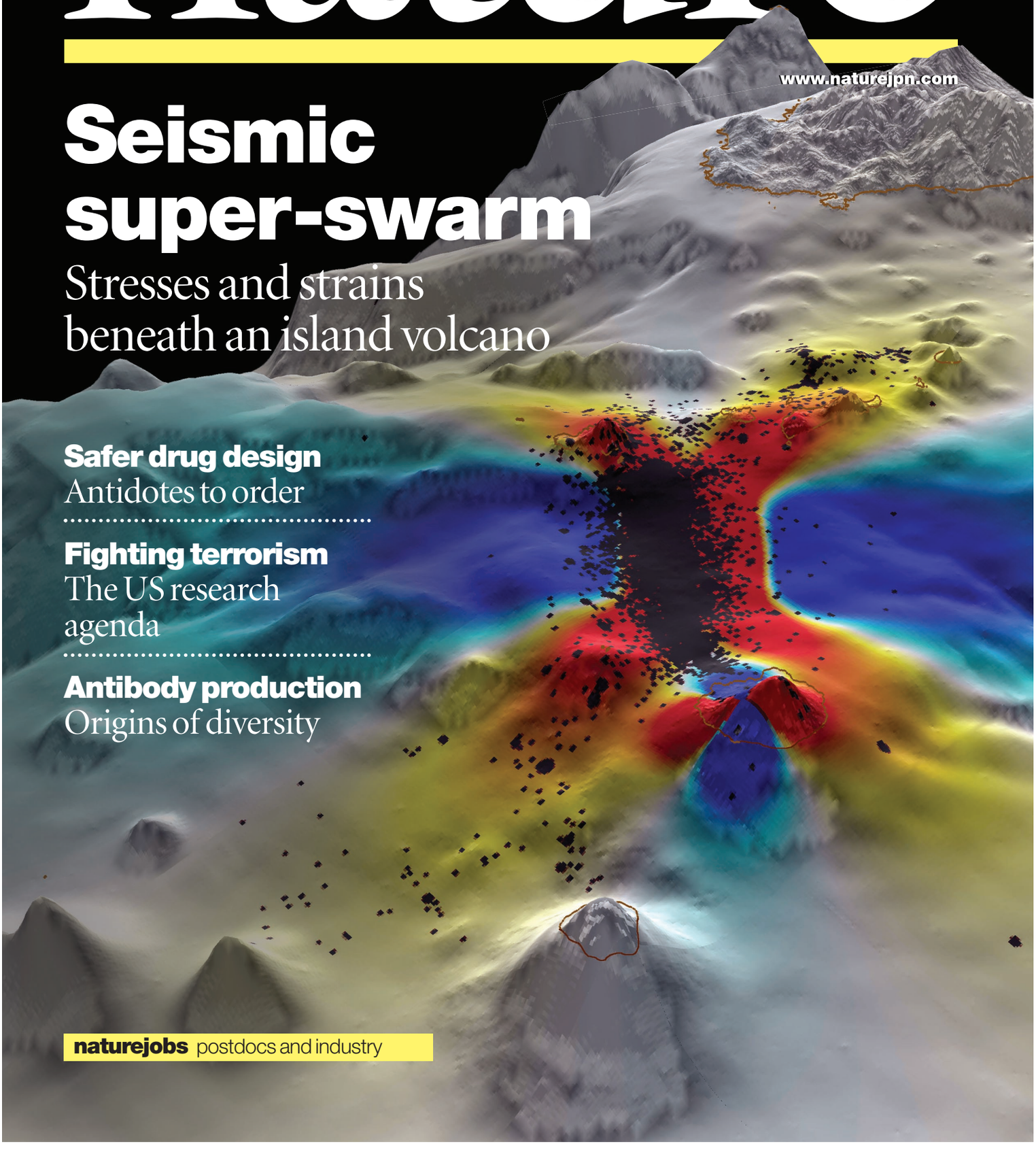

Supplementary Information accompanies the paper on *Nature*'s website (http://www.nature.com/nature).

Acknowledgements

HREM analysis was carried out at the Electron Microscopy Collaborative Research Center at Argonne National Laboratory. This work was supported by the EMSI program of the National Science Foundation and the US Department of Energy Office of Science at the Northwestern University Institute for Environmental Catalysis. M.A. acknowledges funding from the National Science Foundation.

Competing interests statement

The authors declare that they have no competing financial interests.

Correspondence and requests for materials should be addressed to L.D.M. (e-mail: l-marks@northwestern.edu).

Evidence from the AD 2000 Izu islands earthquake swarm that stressing rate governs seismicity

Shinji Toda*, Ross S. Stein† & Takeshi Sagiya‡

** Active Fault Research Center, Geological Survey of Japan, AIST, Tsukuba 305-8567, Japan*
† US Geological Survey, MS 977, Menlo Park, California 94025, USA
‡ Geographical Survey Institute, Tsukuba 305-0811, Japan

Magma intrusions and eruptions commonly produce abrupt changes in seismicity far from magma conduits[1–4] that cannot be associated with the diffusion of pore fluids or heat[5]. Such 'swarm' seismicity also migrates with time, and often exhibits a 'dog-bone'-shaped distribution[3,4,6–9]. The largest earthquakes in swarms produce aftershocks that obey an Omori-type (exponential) temporal decay[10–12], but the duration of the aftershock sequences is drastically reduced, relative to normal earthquake activity[7,13]. Here we use one of the most energetic swarms ever recorded to study the dependence of these properties on the stress imparted by a magma intrusion[8,11,14,15]. A 1,000-fold increase in seismicity rate and a 1,000-fold decrease in aftershock duration occurred during the two-month-long dyke intrusion. We find that the seismicity rate is proportional to the calculated stressing rate, and that the duration of aftershock sequences is inversely proportional to the stressing rate. This behaviour is in accord with a laboratory-based rate/state constitutive law[16], suggesting an explanation for the occurrence of earthquake swarms. Any sustained increase in stressing rate—whether due to an intrusion, extrusion or creep event—should produce such seismological behaviour.

The swarm struck the Izu volcanic islands 150 km south of Tokyo, producing 7,000 shocks with magnitude $M \geq 3$, and five $M \geq 6$ shocks; the total seismic energy release was 1.5×10^4 J, nearly an order of magnitude larger than the swarms that occurred in 1965–67 at Matsushiro, Japan, or in 1980 in Long Valley, California. The Izu swarm was accompanied by five phreatic eruptions of Miyakejima. Seismic activity began on 26 June with a shallow, dense swarm under Miyakejima, and migrated northwest (Fig. 1a). In July, the swarm developed northern and southern lobes (Fig. 1c, d). Earthquakes with $M = 6.4$ (1 July), $M = 6.1$ (9 July) and $M = 6.0$ (18 August) struck near the centre of the swarm, and $M = 6.3$ (15 July) and $M = 6.4$ (30 July) shocks struck ~25 km from the centre. Although it is generally assumed that the duration of aftershock sequences is proportional to mainshock magnitude[10], aftershocks of these $M \approx 6$ strike-slip earthquakes persisted for as little as a day, whereas aftershocks of $M = 6$ events normally last several years in the Izu islands (Fig. 2a). The distance between Kozushima and Shikinejima gradually extended by 0.85 m until 23 August, when the seismicity and rapid displacement ceased[17] (Fig. 3a).

The seismicity and deformation data are most compatible with a laterally propagating dyke intrusion, a process common to the Izu peninsula[8,9,18]. We assume that a vertical dyke propagated to its full length in the first week (Fig. 1a), and then opened continuously for seven weeks. We infer 20 m of expansion over a depth extent of

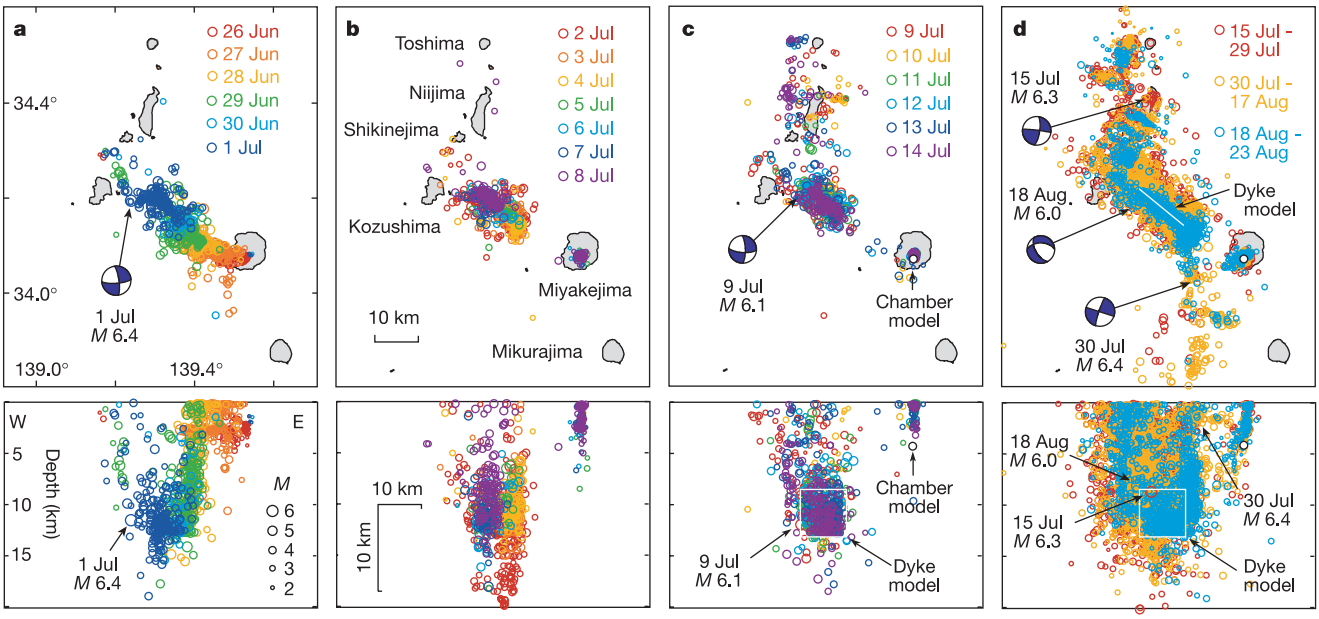

Figure 1 Swarm evolution in map view (top panels) and cross-section (bottom panels). Data from Earthquake Research Institute, University of Tokyo (ERI). Off-dyke seismicity appears within 3 d (**a**), and expands substantially after two weeks (**b**–**d**). Geometry of the inferred dyke and magma chamber is shown in **c**, **d**.

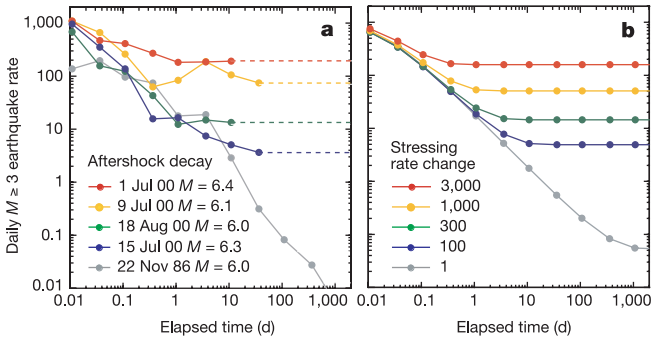

Figure 2 Observed and predicted aftershock decay. **a**, Observed decays for the four largest shocks during the Izu swarm, and for the nearest $M = 6$ shock that occurred well before the swarm (20 km east of Toshima, grey). The 1 July, 9 July and 18 August shocks struck near the dyke; the 15 July shock occurred 20 km north of the dyke. Aftershocks were counted in a 30-km-long cube centred on each hypocentre; curves are dashed after the swarm ended. **b**, Predicted aftershock decay as a function of the stressing rate change. The similarity between **a** and **b** suggests that aftershock decay is controlled principally by the stressing rate. Curves in **b** were generated from equations (12) and (14) in ref. 16, assuming a background stressing rate $\dot{\tau}_r = 0.1$ bar yr^{-1}, $A\sigma_n = 0.1$ bar, and a 1-bar mean stress gain imparted to aftershocks of each $M = 6$ shock. The modelled earthquake rate is given by the stressing rate change times the observed (1980–99) background $M \geq 3$ seismicity rate of 0.05 d^{-1}. The curves are insensitive to the stress change except for the first few hours, but they are sensitive to the background stressing and seismicity rates for longer periods. Stressing rate changes in **b** are chosen to correspond to those estimated for the observed mainshocks in **a**, based on their location, depth, and time of occurrence in the sequence.

Table 1 **Expected number of damaging Izu swarm earthquakes**

Magnitude	Location	Background rate (yr^{-1})	Stressing rate change	Number of shocks	
				Expected*	Observed
$M \geq 6$	Total area	0.09	400	5.8	5
	Near dyke	0.005	3,250	2.6	3
$M \geq 5$	Total area	0.7	400	45	41
	Near dyke	0.04	3,250	21	33

There were seven shocks with $M \geq 6$ from 1926 to 1999 (0.09 yr^{-1}) in the area shown in Fig. 4. The calculated mean swarm stressing rate for this area is 40 bar yr^{-1}, and the background rate is ~0.1 bar yr^{-1}, so the rate change is 400. The 20 km × 20 km near-dyke region comprises the central 6% of the area, so the background rate of near-dyke $M \geq 6$ shocks is 0.005 yr^{-1}.
*Data in this column is given by column 3 entry × column 4 entry × the swarm period (0.16 yr).

8–13 km, and a volume increase of ~1.5 km^3, corresponding to a geodetic moment of ~5×10^{19} N m (Fig. 3b). GPS (Global Positioning System) vectors on Miyake also indicate a magma chamber deflation of 0.12 km^3 at 4 km beneath Miyake during the swarm[17].

We use the dyke expansion model to test whether the swarm seismicity is controlled by stress transferred by the intrusion. Given the background stressing rate (~0.1 bar yr^{-1}) inferred from the strain rate[19], and stressing rates of up to 150 bar yr^{-1} calculated during the intrusion (Fig. 4a), we infer a 1,500-fold gain in the shear stressing rate near the dyke. Seismicity is generally abundant where the stressing rate is calculated to have increased, and rare where it decreased. The calculated stressing rate change (Fig. 4a) is correlated with the observed seismicity rate change (Fig. 4b), suggesting a causal relation.

An alternative hypothesis is that ground water heated by the intrusion diffused outward along pre-existing fractures in the 'dog-bone' lobes, promoting earthquakes by raising pore pressure or temperature. The penetration of the diffusive front is a function of the ratio of the thermal to hydraulic diffusivities[5]. For appropriate values of the thermal (10^{-6} m^2 s^{-1}) and hydraulic (10^{-2} m^2 s^{-1}) diffusivities, the pore pressure increase is negligible beyond 250 m in the first 20 d (ref. 5). Even for highly fractured basalt with permeability as low as 10^{-15} m^2 (ref. 20) at the 5–15 km depth of seismicity, the pulse would reach no more than 2.5 km in 20 d, by which time several $M \approx 6$ shocks and numerous smaller ones had appeared 25 km from the Izu dyke (Fig. 1c, d). Because similar aftershock durations are seen for the events of 18 August (3 km from the dyke) and 15 July (20 km from the dyke), and the decay of the 18 August event is much longer than for the 1 July shock despite a similar proximity to the dyke (Fig. 2a), a temperature dependence of aftershock duration[11] is not evident. Thus, neither pore-fluid nor heat diffusion is likely to explain the remote triggering and shortened aftershock durations at Izu and elsewhere.

In contrast, the stressing-rate dependences of seismicity rate and aftershock duration are properties of a stress transfer model incorporating rate/state friction, for which the seismicity rate

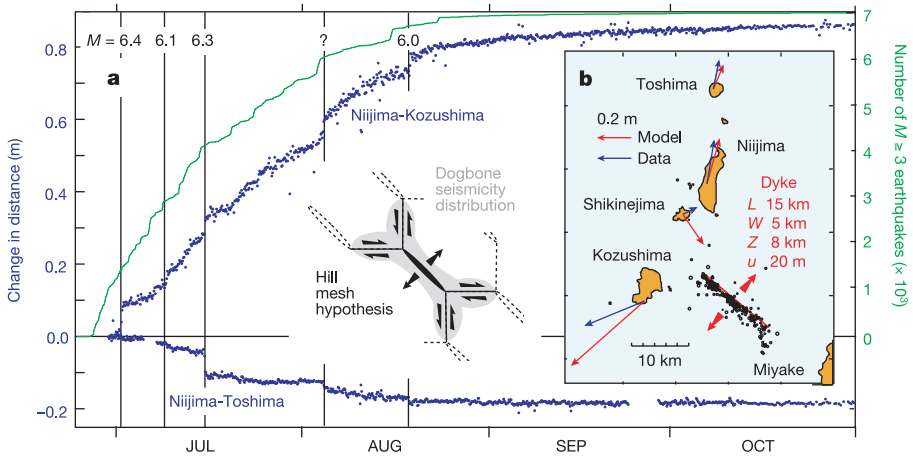

Figure 3 Intrusion geometry and deformation. **a**, GPS line-length changes[17] and cumulative Japan Meteorological Agency (JMA) $M \geq 3$ shocks, with the observed 'dog-bone' pattern (grey) and Hill mesh explanation[6] (black) inset. **b**, We use epicentres at 9–12 km depth located by ocean bottom seismometers to constrain the dyke position[22]; vectors are net displacements; L, length; W, width; Z, upper depth; u, opening. The volume lost to collapse of the summit caldera (0.60 km^3), magma chamber deflation (0.12 km^3), and eruptions (0.02 km^3)[17] is about half that inferred for the dyke intrusion (1.5 km^3), suggesting that some magma migrated from greater depths. The inferred two-month intrusion rate is ~300 m^3 s^{-1}, 10 times that of the 1997 off-Izu intrusion[9].

should be linearly related to the swarm stressing rate (Fig. 5). Although the data are noisy, the observed regression is quite close to the rate/state model (Fig. 4b inset). Aftershock duration t_a, the time until the rate of seismicity returns to what prevailed before the mainshock, is related to shear stressing rate $\dot{\tau}$ by $t_a = A\sigma_n/\dot{\tau}$, where $A\sigma_n$ is a constitutive parameter times the normal stress[16], which we assume to be unchanged by the swarm[15]. The shortened aftershock duration is due to the increased level of background seismicity and to a change in the Omori decay exponent during the swarm (Fig. 2b). Relative to periods without intrusions, aftershock durations should decrease by a factor of ~1,000 above the dyke, and by a factor of ~100 in the off-dyke lobes, in rough accord with the data (Fig. 2a).

The 'dog-bone' pattern of seismicity seen at Izu, and to varying degrees elsewhere[3,4,7–9,18], can be explained by the transfer of shear stress from an expanding dyke to vertical faults in the surrounding crust (Fig. 4a). This pattern, as well as the prevalence of strike-slip focal mechanisms for all but mid-ocean-ridge swarms, were formerly explained by the Hill mesh[6], an hypothesis that strike-slip faults link the dykes, accommodating and transferring the dyke expansion through the mesh (Fig. 3a inset). We instead suggest that seismicity occurs in these lobes whether or not connecting faults exist, and that stress in each lobe can be relieved by right- and left-lateral faulting.

If swarm seismicity is indeed governed by the stressing rate, then the onset and rate of damaging earthquakes in a swarm can be forecast. The expected earthquake rate is the product of the stressing rate change, the background rate for shocks of a given magnitude, and the swarm duration. Retrospective agreement is good for both $M \geq 5$ and $M \geq 6$ Izu shocks (Table 1). Because seismicity reaches equilibrium more slowly at lower stressing rates (Fig. 5b), earthquakes appear to migrate away from the dyke. The near-dyke shocks should start within days of the intrusion (the first $M \geq 6$ shock struck 5 d into the swarm), whereas those off the dyke should be delayed by several weeks ($M \geq 6$ shocks began there after 20 d). The observed rate of seismicity migration is thus more consistent with stress transfer than with pore-fluid diffusion.

Whereas several previous studies have assumed that rate/state friction controls earthquake occurrence[15,21], the voluminous burst of earthquakes at Izu provides the strongest observational test yet of this constitutive law for the genesis of seismicity. Rate/state stress transfer furnishes a comprehensive explanation for distributed swarm seismicity, triggering and clustering, and offers the prospect that near-real-time analysis of seismic and GPS data may permit

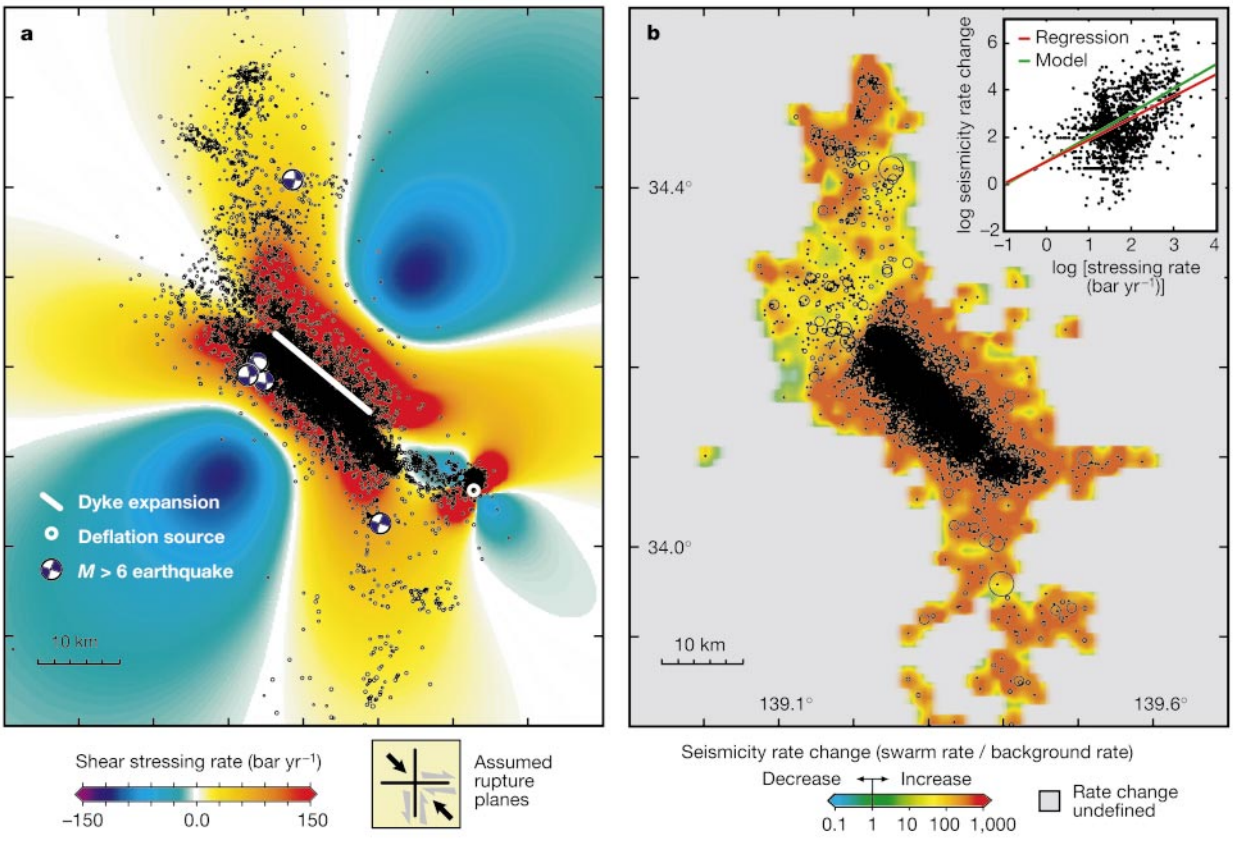

Figure 4 Calculated shear stressing rate and observed seismicity rate. **a**, Shear stressing rate caused by dyke expansion and Miyake deflation (modelled using Coulomb 2.2 (ref. 21) at depths of 2–8 km resolved on vertical planes, consistent with focal mechanisms). Seismicity (ERI, 26 June to 23 August 2000) is more common where the stressing rate is calculated to have increased. **b**, Seismicity rate change[21] smoothed with a 1-km gaussian smoothing radius. The JMA catalogue is used because it is complete to $M \geq 3$ from 1985; 'swarm' is 59 d after 29 June 2000; 'background' is 15 yr before 29 June 2000. The average background rate was substituted for sites with at least one swarm shock but no background seismicity. The brevity of the swarm all but precludes observation of seismicity rate decreases. The inset shows the spatial regression of **a** on **b**. The model (green) is found by combining equations (10) and (11) from ref. 16, for which $R/r = \dot{\tau}/\dot{\tau}_r$ once γ, the state variable for seismicity, reaches steady state; R and $\dot{\tau}$ are the swarm seismicity and stressing rates; r and $\dot{\tau}_r$ are the background seismicity and stressing rates. The model predicts $y = 1.0 \log x + 1.0$; the linear regression (red) yields $y = 0.93 \log x + 0.95$ with correlation coefficient 0.48, significant at the 99.99% confidence level for the effective number of observations (542). Synthetic seismicity with the property that the seismicity rate decreases inversely with distance from the dyke exhibits a much poorer fit to the rate/state model ($y = 0.34 \log x + 2.6$), with slope one-third of the observations or model. The correlation coefficient for the synthetic data regression is <0.75, but depends principally on the amount of introduced noise.

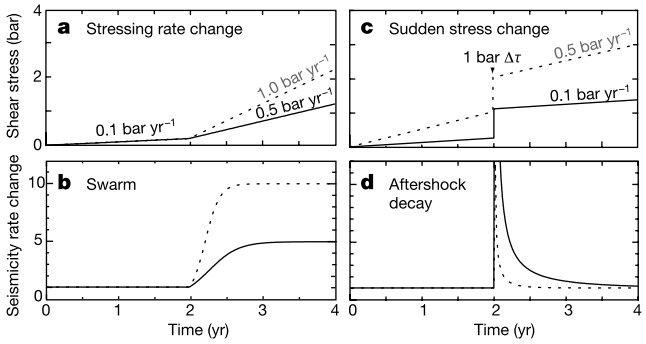

Figure 5 The rate/state effect of stress on seismicity. Details of the calculations are given in Methods. A change in the stressing rate (**a**) causes a swarm (**b**). A sudden stress change, $\Delta\tau$ (**c**), causes an aftershock sequence that decays inversely with time (**d**). The Izu swarm has several aftershock sequences embedded in it. Comparison of dashed and solid curves shows that the higher the stressing rate, the more quickly the seismicity rate reaches equilibrium. As the stressing rate change is highest close to the source, swarm seismicity appears to migrate away from an intrusion or creep site.

forecasts of damaging earthquakes during future swarms. Equally important, the Izu test suggests that a central unresolved problem of earthquake interaction—the response of seismicity to a large shock followed by viscoelastic rebound—is essentially a sudden stress change succeeded by a transient stressing rate change, which can be simulated by combining the two processes shown in Fig. 5. □

Methods

To calculate the updated daily seismicity rate, R, due to a stressing rate change (Fig. 5b), we seek the updated state variable γ from equation (11) of ref. 16, $R = r/(\gamma\dot{\tau}_r)$, where $\dot{\tau}_r$ is the background stressing rate, and the background seismicity rate r is set to 1. At $t = 0$, γ is steady state, where $\gamma_{ss} = 1/(\dot{\tau}_r)$. To evolve γ, we use equation (B17) of ref. 16, $\gamma = \left[\gamma_0 - \frac{1}{\dot{\tau}}\right]\exp\left[\frac{-t\dot{\tau}}{A\sigma_n}\right] + \frac{1}{\dot{\tau}}$, where γ_0 is the state variable before each time step, and $\dot{\tau}$ is the stressing rate. For the response to a sudden stress change $\Delta\tau$ (Fig. 5d), $\gamma = \gamma_0 \exp\left(\frac{-\Delta\tau}{A\sigma_n}\right)$, modified from equation (B11) in ref. 16. For the Izu swarm, we infer $A\sigma_n$ using the relation $A\sigma_n = t_a\dot{\tau}$. From Fig. 2a, t_a for the $M \approx 6$ shocks close to the dyke is ~0.3 d where the calculated stressing rate $\dot{\tau} \approx 150\,\mathrm{bar\,yr^{-1}}$. The observed t_a for the background $M \approx 6$ shock in Fig. 2a is ~1 yr, and the background $\dot{\tau} \approx 0.1\,\mathrm{bar\,yr^{-1}}$. Both estimates yield $A\sigma_n \approx 0.1$ bar, which we use here. The mean stressing rate in Fig. 4a is $32\,\mathrm{bar\,yr^{-1}}$, and the mean t_a for the $M \approx 6$ shocks is ~3 d, for $A\sigma_n \approx 0.3$ bar, similar to a previous estimate[21].

Received 16 April; accepted 19 July 2002; doi:10.1038/nature00997.

1. Weaver, C. S., Grant, W. C., Malone, S. D. & Endo, E. T. The 1980 eruptions of Mt. St. Helens, Washington. *US Geol. Surv. Prof. Pap.* **1250,** 109–121 (1981).
2. Mori, J., Eberhart-Phillips, D. & Harlow, D. H. *Fire and Mud: Eruptions and Lahars of Mount Pinatubo, Philippines* (eds Newhall, C. G. & Punongbayan, R. S.) 371–382 (Univ. Washington Press, Seattle, 1996).
3. Björnsson, A., Saemundsson, K., Einarsson, P. & Tryggvason, E. Current rifting episode in north Iceland. *Nature* **266,** 318–323 (1977).
4. Dvorak, J. J. *et al.* Mechanical response of the south flank of Kilauea Volcano, Hawaii, to intrusive events along the rift systems. *Tectonophysics* **124,** 193–209 (1986).
5. Delaney, P. T. Rapid intrusion of magma into wet rock: Groundwater flow due to pore pressure increases. *J. Geophys. Res.* **87,** 7739–7756 (1982).
6. Hill, D. A model for earthquake swarms. *J. Geophys. Res.* **82,** 1347–1352 (1977).
7. Klein, F. W., Einarsson, P. & Wyss, M. The Reykjanes peninsula, Iceland, earthquake swarm of September 1972 and its tectonic significance. *J. Geophys. Res.* **82,** 865–888 (1977).
8. Ukawa, M. & Tsukahara, H. Earthquake swarms and dike intrusions off the east coast of Izu peninsula, central Japan. *Tectonophysics* **253,** 285–303 (1996).
9. Aoki, Y., Segall, P., Kato, T., Cervelli, P. & Shimada, S. Imaging magma transport during the 1997 seismic swarm off the Izu peninsula, Japan. *Science* **286,** 927–930 (1999).
10. Watanabe, K. On the duration time of aftershock activity. *Bull. Disast. Prev. Res. Inst. Kyoto Univ.* **39,** 1–21 (1989).
11. Kisslinger, C. & Jones, L. Properties of aftershock sequences in southern California. *J. Geophys. Res.* **96,** 11947–11958 (1991).
12. Gross, S. J. & Kisslinger, C. Tests of models of the aftershock rate decay. *Bull. Seismol. Soc. Am.* **84,** 1571–1579 (1994).
13. Walter, A. W. & Weaver, C. S. Seismicity of the Coso Range, California. *J. Geophys. Res.* **85,** 2441–2458 (1980).
14. Chouet, B. A. Long-period volcano seismicity: its source and use in eruption forecasting. *Nature* **380,** 309–316 (1996).
15. Dieterich, J., Cayol, V. & Okubo, P. The use of earthquake rate changes as a stress meter at Kilauea volcano. *Nature* **408,** 457–460 (2000).
16. Dieterich, J. A constitutive law for rate of earthquake production and its application to earthquake clustering. *J. Geophys. Res.* **99,** 2601–2618 (1994).
17. Nishimura, T. *et al.* Crustal deformation caused by magma migration in the northern Izu Islands, Japan. *Geophys. Res. Lett.* **28,** 3745–3748 (2001).
18. Okada, Y. & Yamamoto, E. A model for the 1989 seismo-volcanic activity off Ito, central Japan, derived from crustal movement data. *J. Phys. Earth* **39,** 177–195 (1991).
19. Sagiya, T., Miyazaki, S. & Tada, T. Continuous GPS array and present-day crustal deformation of Japan. *Pure Appl. Geophys.* **157,** 2303–2322 (2000).
20. Ingebritsen, S. E. & Sanford, W. E. *Groundwater in Geologic Processes* 16 (Cambridge Univ. Press, Cambridge, 1998).
21. Toda, S., Stein, R. S., Reasenberg, P. A. & Dieterich, J. H. Stress transferred by the $M_w = 6.5$ Kobe, Japan, shock: Effect on aftershocks and future earthquake probabilities. *J. Geophys. Res.* **103,** 24543–24565 (1998).
22. Sakai, S. *et al.* Magma migration from the point of view of seismic activity in the volcanism of Miyakejima Island in 2000. *J. Geogr.* **110,** 145–155 (2001).

Supplementary Information accompanies the paper on *Nature*'s website (http://www.nature.com/nature).

Acknowledgements

We thank J. Dieterich for guidance and insight; V. Cayol, B. Chouet, D. Hill and W. Thatcher for comments and suggestions; and M. Kikuchi, Y. Yamanaka, S. Sakai and H. Tsuruoka for help in the initial stages of this study. We used ERI, JMA and GSI data, and seismicity-rate computer codes by P. Reasenberg.

Competing interests statement

The authors declare that they have no competing financial interests.

Correspondence and requests for materials should be addressed to S.T. (e-mail: s-toda@aist.go.jp).

Pretender punishment induced by chemical signalling in a queenless ant

Thibaud Monnin*†, Francis L. W. Ratnieks*, Graeme R. Jones‡ & Richard Beard‡

* *Laboratory of Apiculture and Social Insects, Department of Animal and Plant Sciences, University of Sheffield, Sheffield S10 2TN, UK*
‡ *Chemical Ecology Group, School of Chemistry and Physics, University of Keele, Keele, Staffordshire ST5 5BG, UK*

Animal societies are stages for both conflict and cooperation. Reproduction is often monopolized by one or a few individuals who behave aggressively to prevent subordinates from reproducing (for example, naked mole-rats[1], wasps[2] and ants[3]). Here we report an unusual mechanism by which the dominant individual maintains reproductive control. In the queenless ant *Dinoponera quadriceps*, only the alpha female reproduces. If the alpha is challenged by another female she chemically marks the pretender who is then punished[4] by low-ranking females. This cooperation between alpha and low-rankers allows the alpha to inflict punishment indirectly, thereby maintaining her reproductive primacy without having to fight.

Queenless ponerine ants have evolutionarily lost the morphological queen caste[5]. All females are workers who can potentially mate and reproduce sexually (mated workers are called gamergates)[5]. Colonies of *D. quadriceps* have, on average, 80 adult workers and a single gamergate[6], who has the alpha rank in a near-linear dominance hierarchy of about 3–5 high-ranking workers[7]. High-rankers are hopeful reproductives. They do little work, and one of them, usually the beta, replaces the gamergate if she dies[7]. Workers with lower ranks work, and are little involved in dominance

† Present address: Laboratoire d'écologie CNRS UMR 7625, Université Pierre et Marie Curie, 7 quai Saint Bernard, 75 005 Paris, France.

Seismology

Stressed to quaking point

Chris Marone

The Earth's crust can deform catastrophically in earthquakes, but it's difficult to predict exactly what causes such failure. Analysing thousands of small shocks might help us better understand how earthquakes occur.

In the study of earthquake mechanics, one of the biggest problems is pinning down the initial conditions. The slip history and the initial stress field around a fault are rarely known with certainty, making it tricky at best to work out what conditions trigger an earthquake. Uncertainty over fault conditions limit hypothesis-testing and hamper both fundamental studies of earthquake physics and empirical attempts to predict earthquakes. Toda and colleagues[1] (page 58 of this issue) now report a new way to circumvent this problem. Rather than relying on estimates of the absolute stress state, they use the rate of stressing to study earthquake nucleation and seismic deformation. They find that regions stressed at higher rates experience more earthquakes in a given period, in agreement with fault-friction theory[2].

Toda *et al.* used a dense network of seismometers in the Izu Islands volcanic chain, south of Tokyo (Fig. 1), and a seismic catalogue extending back to 1980 to measure changes in the rate of earthquake occurrence around one of the most seismically energetic magma intrusions ever known[3] — in 2000 the region was hit by a 'swarm' of more than 7,000 shocks. The authors infer that a vertical fracture, 8 km below the surface and 5 km × 15 km in area, was forcibly expanded to a width of 20 m by magma intrusion at an average rate of 300 $m^3 s^{-1}$ during a two-month period. In some areas the local stressing rate increased by a factor of up to 1,500 relative to the background rate. By comparing seismic activity before and after the intrusion, the authors find that earthquake rates jumped by a factor of nearly 1,000 in the areas of highest stressing rate, some locations suffering daily the equivalent of 1,000 earthquakes of magnitude 3 or more. They also show that the rate of seismic activity decreases in areas where the stressing rate decreases, in agreement with previous work[4].

KYODO NEWS

Figure 1 **Miyakejima, Izu Islands, August 2000. Mount Oyama erupts as the islands suffer thousands of earthquakes.**

Significant in the work of Toda *et al.*[1] is their use of earthquake observations to test seismicity–rate theory[2] and the laboratory-derived friction laws[5] on which it is based. The friction laws indicate that fault strength is not well described by a simple stress threshold but rather is a function of strain rate and recent slip history — that is, the 'frictional state'. History- or state-dependence of friction accounts for time-dependent strengthening of frictional contacts and for the fact that a finite displacement is necessary for the frictional resistance to make a transition from one set of conditions to another — for example, from stationary to sliding contact, or from steady sliding at one velocity or normal stress to another. Friction rate and state effects are well documented in laboratory experiments; however, testing how well they apply to earthquake faults has proved difficult and controversial.

At issue is whether the same processes that occur under laboratory conditions also govern seismic failure in the field, because the latter may involve slip rates of up to several metres per second and significant shear heating. Although the laboratory laws can reproduce much observed fault behaviour (including slow earthquakes, aseismic strain transients, dynamic rupture and interseismic fault healing[5,6]), the stumbling block is that numerical simulations of these phenomena in the field must generally use parameter values that differ from those measured in the laboratory. Seismic and geodetic observations can rarely specify friction values with sufficient precision to resolve the discrepancy. But Toda *et al.* have devised a different type of test, combining field-based estimates of the friction parameters with laboratory-based predictions of seismic behaviour.

Dieterich's seismicity–rate theory[2] predicts that a stress perturbation vanishes sooner if the background stressing rate is higher. As aftershocks are a product of the stress perturbation generated by the main shock, their duration — the time for the seismicity to return to the pre-mainshock level — should scale inversely with stressing rate. The Izu Islands swarm includes five magnitude-6 earthquakes, and Toda *et al.* record a strong inverse correlation between aftershock duration and stressing rate: aftershocks of magnitude-6 earthquakes, which would normally go on for several years, lasted only a day in the areas of highest stressing rate.

This agreement between theory and observation is a significant step forward for earthquake mechanics. The seismicity–rate theory also predicts a relationship between aftershock duration, stressing rate, and a friction parameter that describes the instantaneous friction response to a step change in slip velocity. Modelling studies show that larger values of the friction parameter prolong the time needed to reach instability[7]; hence, aftershock duration increases with the friction parameter. Laboratory experiments[8] show that the parameter (which is always positive) is between 10^{-3} and 10^{-2}, in good agreement with the value obtained by Toda *et al.*[1] from measured aftershock durations and stressing rates.

Seismicity–rate theory also predicts that a change in stress level will have a markedly different effect from a change in stressing rate, and Toda *et al.* show how this could improve understanding of postseismic behaviour. The main shock of an earthquake increases the stress around a rupture, but this increase decays rapidly because the brittle crust behaves as a stiff elastic material. In contrast, the effective stiffness is expected to be significantly lower in some cases, including large earthquakes that rupture into the frictionally viscous region below the seismogenic zone. Toda *et al.* note that the combined effects of a jump in stress level and stressing rate could help explain transient behaviour observed after large earthquakes.

Given the issues discussed above, it is clearly difficult to predict details of a particular earthquake, including when and where it may nucleate. But the method of Toda *et al.* presents an opportunity to test earthquake theories that could lead the way to fundamental breakthroughs. The correlation between stressing rate and seismicity may help in forecasting swarm or aftershock damage; however, there is still the problem of rupture size and understanding how earthquakes stop. Because large earthquakes appear to be seismically identical to small shocks, forecasts and damage predictions will remain limited, at least for the moment, to minimum estimates. ■

Chris Marone is in the Department of Geosciences, 536 Deike Building, The Pennsylvania State University, University Park, Pennsylvania 16802, USA.

e-mail: cjm@essc.psu.edu

1. Toda, S., Stein, R. S. & Sagiya, T. *Nature* **419,** 58–61 (2002).
2. Dieterich, J. H. *J. Geophys. Res.* **99,** 2601–2618 (1994).
3. http://sicarius.wr.usgs.gov
4. Dieterich, J. H., Cayol, V. & Okubo, P. *Nature* **408,** 457–460 (2000).
5. Marone, C. *Annu. Rev. Earth Planet. Sci.* **26,** 643–696 (1998).
6. Scholz, C. H. *Nature* **391,** 37–42 (1998).
7. Roy, M. & Marone, C. *J. Geophys. Res.* **101,** 13919–13932 (1996).
8. Blanpied, M. L., Marone, C., Lockner, D. A., Byerlee, J. D. & King, D. P. *J. Geophys. Res.* **103,** 9691–9712 (1998).